

Structure–property relations in a hypereutectic aluminium–silicon alloy dispersed with graphite particles

B.K. PRASAD

Regional Research Laboratory, Council of Scientific and Industrial Research, Bhopal 462 026, Madhya Pradesh, India

Changes in the microstructure and properties of an Al–Si (BS LM30) alloy dispersed with graphite particles brought about by T6 (solutionizing followed by artificial ageing) treatment were investigated. A range of ageing temperatures such as 165, 180, 215 and 240 °C were selected while the soaking time was varied from 1–24 h with a view to optimize the parameters. The base alloy processed under identical conditions was also heat treated, together with the composite to understand the role of the dispersoid in the alloy. Their properties, such as hardness, density and electrical resistivity were determined. Corresponding microstructural changes as a function of ageing temperature and duration were also observed. Observations made in this study indicate that the hardness peak shifted towards shorter soaking periods with temperature. The base alloy and the composite were found to follow a similar trend. However, the former possessed higher hardness and density and lower electrical resistivity. The changes in properties of the specimens were supplemented with considerable morphological modification of the matrix, the latter included the spheroidization of eutectic silicon particles and complex intermetallic compounds together with reduction in the size of the primary silicon phase due to fragmentation and dissolution. The study suggests that the heat treatment has tremendous potential to produce a desired combination of matrix microstructure and properties in graphitic Al–Si alloys by varying the treatment parameters, e.g. temperature and duration.

1. Introduction

Graphitic aluminium alloys have been found to be potential engineering materials for a variety of anti-friction and antiwear applications [1–5]. In such applications, the presence of graphite in Al–Si alloys ensures smooth functioning in service under the conditions of boundary lubrication which are encountered sometimes due to the temporary scarcity of the lubricant. A recent study [6] has indicated that there is a wide scope for improving the friction and wear properties of the graphitic aluminium–silicon alloys by heat treatment. In addition to this, it is also possible to compensate for the deterioration in their properties, such as hardness, strength etc., to some extent by the heat treatment; the deterioration in the properties of the composites occurs due to the presence of the weaker graphite particles [7]. This requires the selection of a heat-treatable variety of Al–Si alloy matrix for dispersing the graphite particles. Elements like copper, nickel, magnesium, etc., when present in the binary Al–Si alloys, make the latter heat treatable [8].

T6 treatment is one of the widely used heat treatments for aluminium-based alloys. Optimization of the temperature and duration of the treatment plays an important role towards obtaining a good combina-

tion of the matrix microstructure and mechanical and tribological properties of the alloys. Thus, although the T6 treatment has great potential towards improving the mechanical and tribological properties of the graphitic aluminium alloys, very limited information is available on the subject [6]. Further, no systematic study has been made.

In view of this, the present investigation was carried out to determine the response of a heat-treatable hypereutectic Al–Si (BS LM30) alloy dispersed with 3.0 wt% graphite particles over a range of ageing temperatures and times in terms of structure–property related changes. The treatment parameters, such as temperature and time, have been optimized for the base alloy and the composite. The influence of adding graphite to the base alloy was also examined.

2. Experimental procedure

2.1. Composite preparation

The composite was prepared by dispersing heat-treated uncoated graphite particles (size 45–150 µm) on the vortex of the base alloy (BS LM30 Al–17.0Si–4.5Cu–0.5Mg–0.1Ni–0.3Fe–0.1Mn) melt. A mechanical stirrer was used to create the vortex.

This was followed by casting the composite melt in permanent moulds in the form of 20 mm diameter, 150 mm long cylindrical bars. The base alloy was also cast in the same moulds.

2.2. Heat treatment

Small (20 mm diameter, 10 mm long) specimens were cut from the cast bars and solution treated at 510 °C for 7 h. The selection of the mentioned solution treatment temperature and time was based on an optimization study carried out earlier [9]. The solution-treated specimens were then aged at various temperatures, such as 165, 180, 215 and 240 °C for a wide range (1–24 h) of times. Water quenching was adopted in order to bring the specimens from the treatment temperatures to room temperature.

2.3. Specimen preparation

Specimens for microstructural observations and property evaluation were polished according to standard metallographic techniques. Keller's reagent was used for etching the samples. Microstructural investigations were carried out using a Leitz optical microscope.

2.4. Measurement of properties

Hardness, electrical resistivity and density of the base alloy, as well as the composite in as-cast and heat-treated conditions, were determined. Reported values represent an average of six observations.

A Brinell hardness tester was used to measure the hardness of the specimens. Electrical resistivity of the samples was determined by converting the corresponding electrical conductivity values measured with the help of a Technofour type 757 conductivity meter. The water-displacement technique was adopted to determine the density of the base alloy and composite. A Mettler microbalance was used to weigh the specimens in order to evaluate the density.

3. Results

Fig. 1 shows the microstructure of the graphitic alloy in the as-cast condition. The dendritic structure of the matrix containing needle-shaped eutectic silicon particles in the interdendritic region and the dispersed graphite particles may be seen in Fig. 1a. An entanglement of typical primary silicon particles with graphite (marked by arrows) may also be seen in the figure. Fig. 1b delineates the needle-shaped (arrowed) intermetallic compound.

The microstructure of the specimens solution treated at 510 °C for 7 h (Fig. 2) revealed significant morphological modifications in the matrix microstructure over that of its as-cast condition (Fig. 1). The microstructural changes included (i) the breaking of the as-cast dendritic structure (Fig. 2a), (ii) the tendency of the eutectic silicon phase towards spheroidization (Fig. 2b), (iii) fragmentation (or a tendency to do so) of the primary silicon particles into smaller

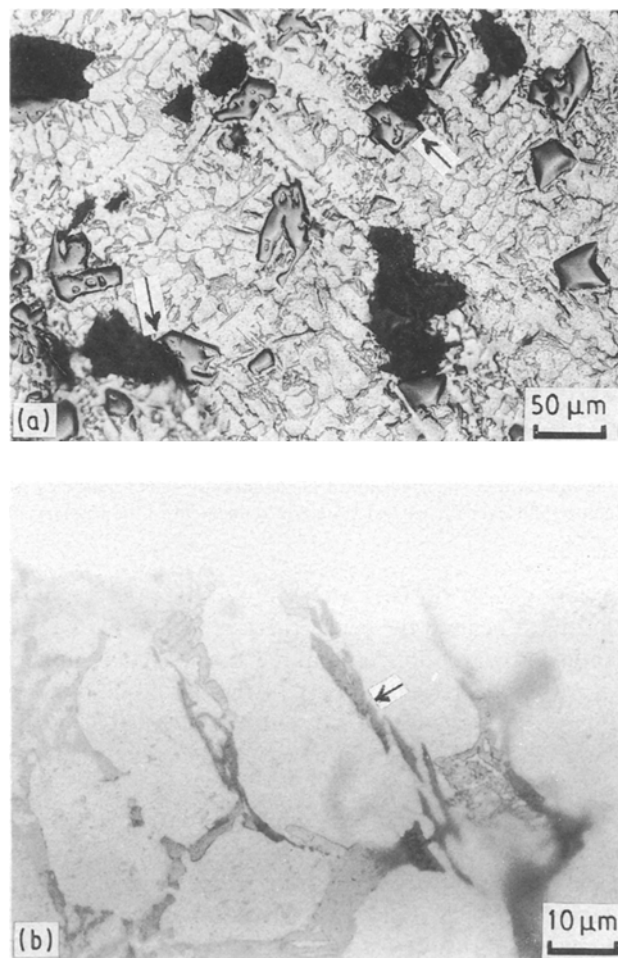


Figure 1 Optical micrographs of the as-cast graphitic LM30 alloy showing (a) the dispersion of graphite particles in the matrix, and (b) the needle-shaped complex intermetallic compound (arrowed). The dendritic structure of the matrix and the entanglement of primary silicon particles with graphite (arrowed) may also be noted in (a).

ones (arrowed in Fig. 2b), and (iv) the modification of the complex intermetallic compound from the as-cast needle shape (arrowed in Fig. 1b) to platelets with blunted edges or semi-rounded ones (Fig. 2b).

Microstructural changes in the composite after ageing at 180 °C for various times are shown in Fig. 3. Fig. 3a and b delineate the increased extent of spheroidization of the microstructural constituents over that of the only solution-treated state of the specimens (Fig. 2). Increasing the ageing time led to the coarsening and thickening of the eutectic silicon and complex intermetallic phases (Fig. 3c).

The region marked by an arrow in Fig. 3a represents another example of the entanglement of the primary silicon phase with graphite. Fragmentation of typical primary silicon particles into smaller ones may also be noted in Fig. 3b (arrowed).

Microstructural observations made at other temperatures of ageing were identical except that the changes occurred at relatively shorter times as the treatment temperature was increased.

The influence of ageing temperature and duration on the hardness of the base alloy with and without the dispersion of graphite particles may be seen in Fig. 4. It may be noted that the hardness of the specimens increased with the ageing time at all the temperatures

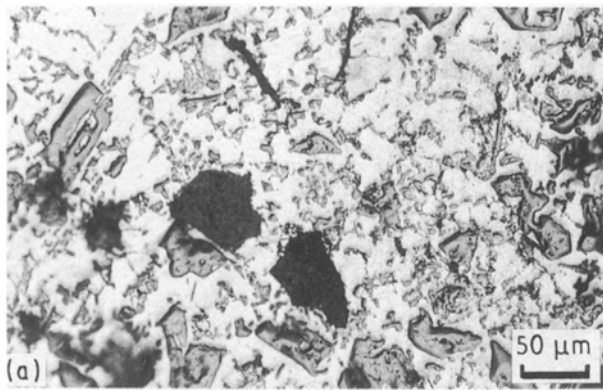


Figure 2 Micrographs of the composite after solution treatment at 516°C for 7 h revealing (a) the breaking of the as-cast dendritic structure of the matrix and spheroidization of the eutectic silicon particles, and (b) the modification in the morphology of the complex intermetallic compound over the as-cast state and refinement of the primary silicon phase through fragmentation (arrowed).

except at 240°C. This was followed by a reduction in hardness beyond the peak. Further, the hardness peak shifted towards longer soaking times as the temperature was decreased (Fig. 4). It was also noted that the composite possessed lower hardness than that of the base alloy and the trend maintained was identical (Fig. 4).

Electrical resistivity of the aged specimens as a function of temperature and time is shown in Fig. 5. A peak in the resistivity at some temperatures was observed (Fig. 5). Further, the composite possessed higher electrical resistivity than the base alloy at all treatment temperatures.

Changes in the density of the samples at different ageing temperatures with time are evident in Fig. 6.

Reduced density of the composite, compared to that of the base alloy in all the ageing conditions, is clearly visible in the figure. Changes in the density of the two kinds of specimens during ageing followed definite but different trends (Fig. 6), although the changes were marginal. It was observed that the density of the base alloy increased initially, while that of the composite decreased (Fig. 6). This was followed by constant density beyond the critical time in both cases, as shown in Fig. 6.

4. Discussion

Entanglement of the primary silicon phase with that of graphite (Figs 1a and 3a) could be attributed to the availability of easy nucleation centres offered by the dispersoid phase to the first solidifying primary silicon particles. The morphological modifications of the microstructural phases of the matrix, such as the spheroidization of the eutectic silicon and the intermetallic compound and the fragmentation of the primary silicon particles, after heat treatment (Figs 2 and

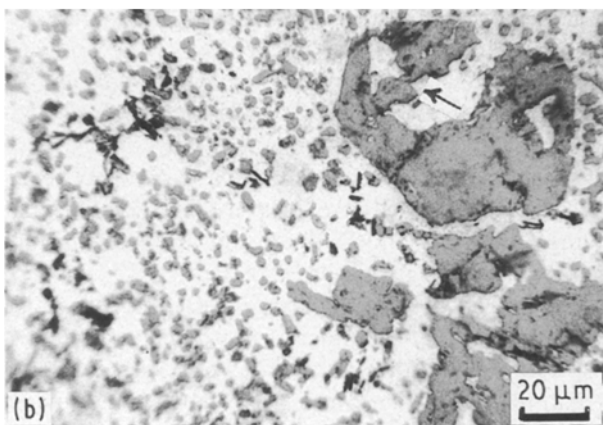
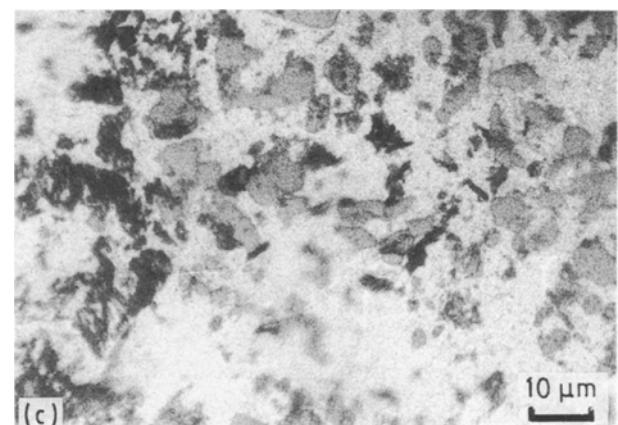


Figure 3 Microstructures of the composite after ageing at 180°C for (a, b) 8 h and (c) 16 h. Increased extent of spheroidization of the eutectic silicon and the complex intermetallic phases (a) and fragmentation of primary silicon particles (arrowed in b) may be noted. A typical example of the entanglement of the primary silicon with graphite is evident in (a) (arrowed) while coarsening of the phases may be seen in (c).



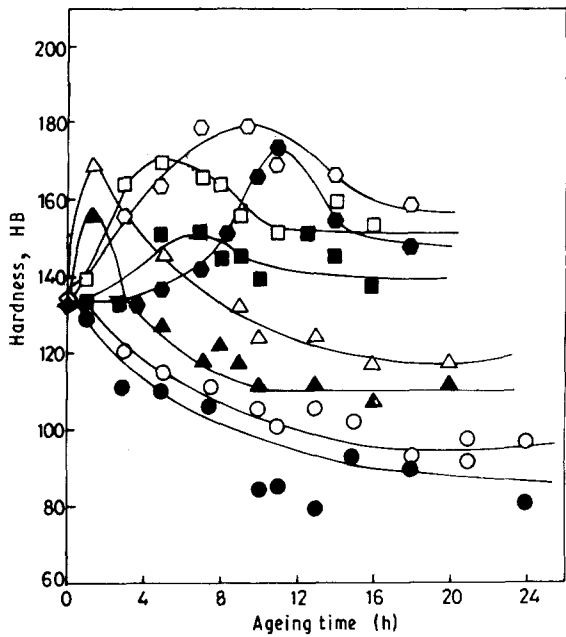


Figure 4 Hardness of the LM30 alloy with (\blacklozenge , \bullet , \blacktriangle , \blacksquare , \bullet) and (\diamond , \circ , \triangle , \square , \circ) without the dispersion of graphite particles as a function of ageing time at various temperatures. (\diamond , \blacklozenge) solution treated, (\circ , \bullet) 240°C, (\triangle , \blacktriangle) 215°C, (\square , \blacksquare) 180°C, (\circ , \bullet) 165°C.

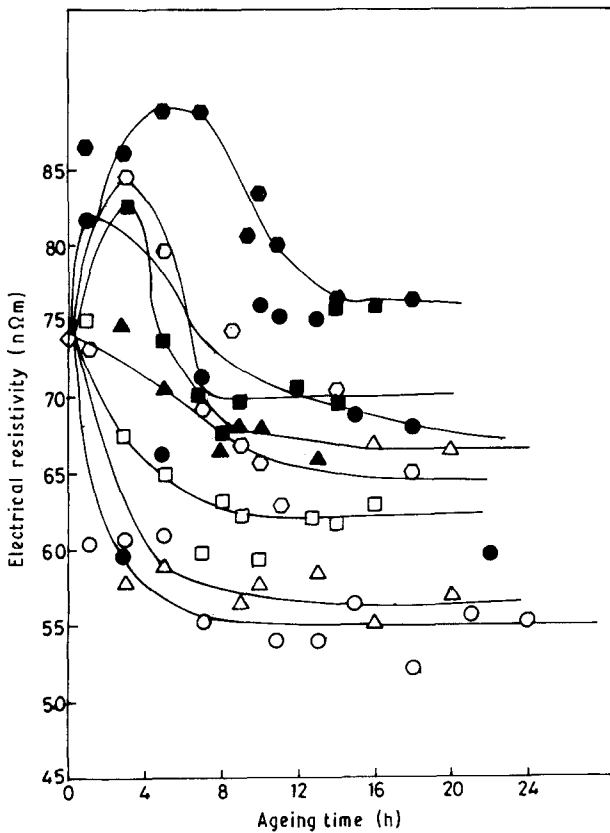


Figure 5 Electrical resistivity of the base alloy and the composite at various ageing times and temperatures. See key to Fig. 4.

3), could be attributed to their dissolution at sharp tips and edges and relatively thinner portions caused by higher elemental concentration gradients there [10].

The increase in the hardness of the specimens with the ageing time prior to attaining the peak (Fig. 4) was the result of spheroidization and refinement of the existing microstructural phases (Fig. 3a and b) and

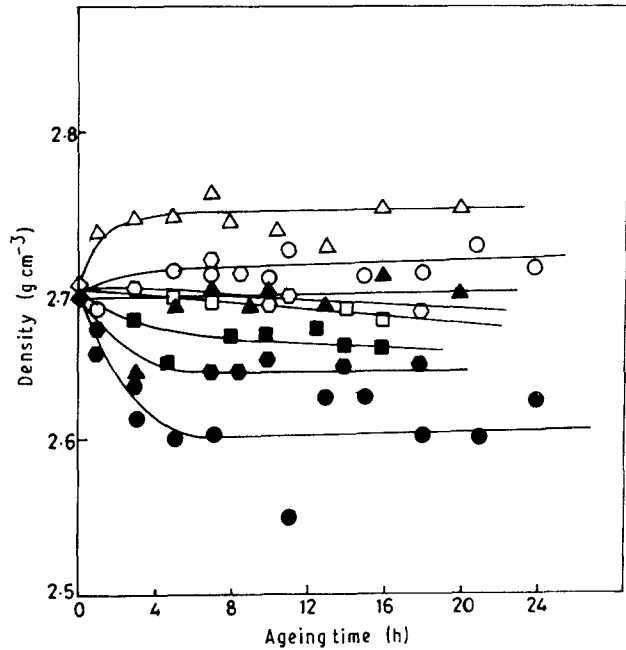


Figure 6 Density of the composite and the base alloy at different times and temperatures of ageing. See key to Fig. 4.

the possible precipitation of other constituents [11]. Coarsening and thickening of the phases (Fig. 3c) was responsible for the reduction in the hardness values of the specimens at longer durations beyond the peak.

Shifting of the hardness peaks towards longer times at lower ageing temperatures (Fig. 4) indicates that the microstructural changes were occurring relatively slowly at the temperatures. The reasons why no hardness peak was observed at 240°C (Fig. 4) suggests that the same effect had occurred before the first measurement was made. Identical trends followed by the alloy with and without graphite dispersion (Fig. 4) agreed well with the fact that the dispersoid forms a mechanical mixture with the aluminium matrix. This suggests that the response of the composite would be governed by its matrix part which was essentially the same as the base alloy.

It is evident that the change in the trend of variation of the electrical resistivity (Fig. 5) and density (Fig. 6) of the composite over the base alloy was due to the presence of graphite particles in the former.

Bearing in mind the partial bonding of graphite with aluminium matrix (Fig. 7), under the conditions of gravity casting [12], it appears that effects such as increased electrical resistivity and reduced density of the composite with ageing time, produced by the swelling of the graphite/matrix interfacial porosity [13], were predominant over the increased density and decreased electrical resistivity of the matrix under identical conditions. Increase in the density and reduced electrical resistivity (Fig. 5) of the aged base alloy over that of its only solution-treated state, although marginal (Fig. 6), could be due to the possible annihilation of lattice defects. However, the reason still needs confirmation.

These observations also indicate that the graphite/aluminium interfacial porosity was able to influence the electrical resistivity and density of the composite to a greater extent than that of its hardness.

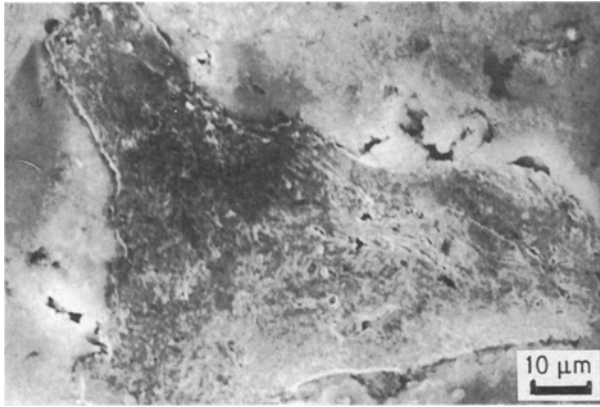


Figure 7 Porosity at the graphite/matrix interface of the gravity die-cast composite.

Heat treatment thus helps towards bringing about significant morphological changes in graphitic Al–Si alloys together with improvement in their properties. This also suggests that it is quite possible to compensate for the deterioration in the properties of the base alloy due to the dispersion of graphite particles. A desired combination of properties and the matrix microstructure could be achieved in graphitic Al–Si alloys by adopting the heat treatment under optimized conditions. Such a combination of microstructure (consisting of spheroidized and refined constituents) and properties has been found to offer improved tribological properties to the alloys.

5. Conclusions

1. Heat treatment of the graphitic aluminium-silicon alloy (BS LM 30) could help to achieve a desired combination of matrix microstructure consisting of spheroidized and refined constituents and improved properties.

2. The optimized heat treatment parameters such as solutionizing at 510 °C for 7 hrs followed by ageing at 165–180 °C for 8–10 hrs offered the best combination of matrix microstructure and hardness. Higher ageing temperatures and durations caused lowering of the hardness due to the coarsening of the microstructural phases, and hence is undesirable.

3. Microstructural modifications during heat treatment resulted from the dissolution of the phases at sharp tips and edges and relatively thinner portions due to a higher elemental concentration gradient in such regions.

References

1. B. C. PAI, P. K. ROHATGI and S. VENKATESH, *Wear* **30** (1974) 117.
2. L. BRUNI and P. IGUERA, *Automot. Engng* **3** (1978) 29.
3. P. K. ROHATGI and B. C. PAI, *Wear* **59** (1980) 373.
4. F. A. BADIA and P. K. ROHATGI, *Trans. Soc. Automot. Engng* **77** (1969) 700.
5. B. P. KRISHNAN, N. RAMAN, K. NARAYANASWAMY and P. K. ROHATGI, *Wear* **20** (1980) 205.
6. S. DAS, S. V. PRASAD and T. R. RAMACHANDRAN, *ibid.* **133** (1989) 173.
7. B. S. MAZUMDAR, A. H. YEGNESWARAN and P. K. ROHATGI, *Mater. Sci. Engng* **68** (1984) 85.
8. J. E. HATCH, "Aluminium: Properties and Physical Metallurgy" (ASM, Metals Park, OH, 1984).
9. B. K. PRASAD and T. K. DAN, *J. Mater. Sci. Lett.*, **10** (1991) 1412.
10. I. NOVIKOV, "Theory of Heat Treatment of Metals" (Mir, Moscow, 1978)
11. G. GUSTAFSSON, T. THORVALDSSON and G. L. DUNLOP, *Met. Trans.* **17A** (1986) 45.
12. B. K. PRASAD, T. K. DAN and P. K. ROHATGI, *J. Mater. Sci. Lett.* **6** (1987) 1076.
13. A. K. JHA, S. V. PRASAD and G. S. UPADHYAYA, *Tribol. Int.* **22** (1989) 321.

Received 1 October 1991
and accepted 17 June 1992